A Moore-Greitzer axial compressor model with spool dynamics.

Jan Tommy Gravdahl and Olav Egeland
Department of Engineering Cybernetics
Norwegian University of Science and Technology
O.S. Bragstads plass 8, N-7034 Trondheim, Norway
Email: {Tommy.Gravdahl,Olav.Egeland}@itk.ntnu.no

Abstract

The compressor stall/surge model of Moore and Greitzer [11] is extended to include the spool dynamics. This results in a model with four states, where the new state is the B-parameter. The effect of a time varying B-parameter on the post stall transients of an axial compressor is demonstrated through simulations of a compression system with speed control.

1 Introduction

The low order model of Moore and Greitzer [11] for the post stall transients of axial compression systems has been used extensively in stall/surge analysis and control. In the original work of Moore and Greitzer, the compressor speed is assumed constant. If the equilibrium of the compression systems is located to the left of the surge line, which passes through the local maxima of the compressor characteristic, the flow becomes unstable. Dependent on certain system parameters, and as will be demonstrated, compressor speed, the instability can take the form of either rotating stall, surge or both. Surge is an axisymmetric oscillation of the flow and rotating stall is characterized by regions of reduced flow that rotates around the annulus of the compressor. These oscillations severely reduces the compressor efficiency and can possibly damage the compressor. A number of approaches to control of surge and rotating stall have been proposed. A review of the different approaches can be found in [1].

In [7] it was concluded that low values of Greitzer's B-parameter B leads to rotating stall, while high values of B leads to surge. As B is proportional to the angular speed of the machine, it is of major concern to stall/surge controller design to include the spool dynamics in a stall/surge-model. A model for centrifugal compressors with nonconstant speed was presented in [2]. In [5] a similar model was derived, and surge and speed control was investigated. However, as the models of [2] and [5] are developed for centrifugal machines, they do not include the equations for rotating stall.

In table 1, the development in stall/surge modeling and control is outlined. In [8] it was demonstrated that the model of [6] also applies to centrifugal compressors. It seems that the modeling and control of an axial compression system including both rotating stall and spool speed is an open problem. The problem is also listed among topics for further research in [7]. In this paper we propose an extension to the Moore/Greitzer model that includes the B-parameter as a state.

Author(s)	states	A/C	M/C/S
Greitzer [6]	Φ, Ψ	A	M
Hansen et.al [8]	Φ, Ψ	C	M
several (see [1]), incl. Gravdahl/Egeland [3]	Φ, Ψ	A/C	C
Moore/Greitzer [11]	Φ, Ψ, J	A	M
several (see [1]), incl. Gravdahl/Egeland [4]	Φ, Ψ, J	A	C
Fink et.al [2]	Φ, Ψ, B	C	M
Gravdahl/Egeland [5]	Φ, Ψ, B	C	MCS
Gravdahl/Egeland (this paper)	Φ, Ψ, J, B	A	MS

Table 1: Development in compressor stall/surge-control. A=Axial, C=Centrifugal, M=Modeling, C=stall/surge control, S=Speed-control

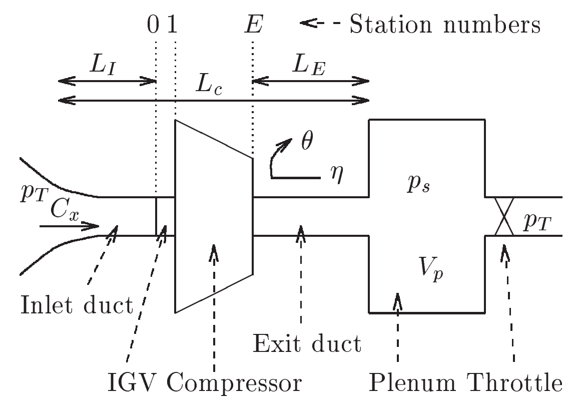

Figure 1: Compression system

2 Preliminaries

The compression system consists of an inlet duct, inlet guide vanes (IGV), variable speed axial compressor, exit duct, plenum volume and a throttle. The throttle can be regarded as a simplified model of a turbine. The system is shown in figure 1. Our aim is to develop a model for this system in the form

$$\dot{\boldsymbol{z}} = \boldsymbol{f}(\boldsymbol{z}), \tag{1}$$

where $\boldsymbol{z} = (\Phi,\ \Psi,\ J,\ B)^{\mathrm{T}}$ and Φ is the circumferentially averaged flow coefficient, Ψ is the total-to-static pressure rise coefficient, J is the squared amplitude of angular variation (rotating stall) and B is Greitzer's B-parameter, which is proportional to the speed of the compressor. The modeling of the compression system relies heavily on the modeling in [11], however the assumption of constant angular speed ω, and thus constant B, is relaxed and a momentum balance for the spool is included. In [11] nondimensional time was defined as

$$\xi_{MG} = \frac{Ut}{R}, \tag{2}$$

where U is the spool speed at mean radius, R is the mean compressor radius and t is time. As we in this paper consider time varying U, this normalization will not be used. Instead we propose to use

$$\xi = \frac{U_d t}{R}, \tag{3}$$

where U_d is the *desired* constant velocity of the wheel. Note that if $U_d = U = const$, we have that $\xi = \xi_{MG}$. All distances are nondimensionalized wrt R, that is the nondimensional duct lengths, are defined as

$$l_I = \frac{L_I}{R} \text{ and } l_E = \frac{L_E}{R}. \tag{4}$$

The axial coordinate is denoted η and the circumferential coordinate is the wheel angle θ. Greitzer's B-parameter is defined as

$$B \triangleq \frac{U}{2a_s}\sqrt{\frac{V_p}{A_c L_c}}, \tag{5}$$

where a_s is the speed of sound, V_p is the plenum volume, A_c is the compressor duct flow area and L_c is the total length of compressor and ducts. B and U is related as

$$U = bB, \text{ where } b \triangleq 2a_s\sqrt{\frac{A_c L_c}{V_p}}. \tag{6}$$

3 Modeling

3.1 Spool dynamics

The momentum balance of the spool can be written

$$I\frac{d\omega}{dt} = \tau_t - \tau_c, \tag{7}$$

where ω is the angular speed, I is the spool moment of inertia, and τ_t and τ_c are the drive (turbine) torque and compressor torque respectively. Using $\omega = 2U/R$, (3) and (5), the spool dynamics (7) can be written

$$\frac{4a_s I U_d}{R^2}\sqrt{\frac{A_c L_c}{V_p}}\frac{dB}{d\xi} = \tau_t - \tau_c. \tag{8}$$

As in [2], torques are nondimensionalized according to

$$\Gamma = \Gamma_t - \Gamma_c = \frac{\tau_t - \tau_c}{\rho A_c R U^2}, \tag{9}$$

where ρ is the constant inlet density. Now, equation (8) can be written

$$\frac{dB}{d\xi} = \Lambda_1 B^2(\Gamma_t - \Gamma_c), \tag{10}$$

where the constant Λ_1 is defined as

$$\Lambda_1 \triangleq \frac{\rho R^3 A_c}{2IU_d}b. \tag{11}$$

As the compressor torque equals the change of angular momentum of the fluid [9], the compressor torque can be written

$$\tau_c = m_c R_{tip} C_{tip}, \tag{12}$$

where R_{tip} is the radius of the rotor and C_{tip} is the tangential velocity of the fluid as it leaves the rotor. Using the slip factor

$$\sigma \triangleq \frac{C_{tip}}{U_{tip}}, \tag{13}$$

equation (12) can be written

$$\tau_c = \sigma m_c \frac{R_{tip}^2}{R}U. \tag{14}$$

For simplicity, the inlet tangential velocity of the gas has been ignored in τ_c. The compressor mass flow is given by

$$m_c = \rho A_c U \phi. \tag{15}$$

Combining (12) and (15) gives

$$\tau_c = \sigma\rho A_c \frac{R_{tip}^2}{R}U^2\phi, \tag{16}$$

and by (9) the nondimensional compressor torque is

$$\Gamma_c = \sigma\left(\frac{R_{tip}}{R}\right)^2\phi. \tag{17}$$

3.2 Compressor

The pressure rise over a single blade row is [10]

$$\frac{p_E - p_1}{\frac{1}{2}\rho U^2} = F(\phi) - \tau\frac{d\phi}{dt}, \tag{18}$$

where

$$\phi = \frac{C_x}{U} \tag{19}$$

is the local axial flow coefficient, $F(\phi)$ is the pressure rise coefficient in the blade passage and τ is a coefficient of pressure rise lag. According to [11], $\frac{d\phi}{dt}$ can be calculated as

$$\frac{d\phi}{dt} = \left(\frac{\partial\phi}{\partial t}\right)_{rotor} + \left(\frac{\partial\phi}{\partial t}\right)_{stator}. \tag{20}$$

Using (3) it is seen that

$$\begin{aligned}\left(\frac{\partial\phi}{\partial t}\right)_{rotor} &= \frac{\partial\phi}{\partial\xi}\frac{\partial\xi}{\partial t} + \frac{\partial\phi}{\partial\theta}\frac{\partial\theta}{\partial t} \\ &= \frac{U_d}{R}\frac{\partial\phi}{\partial\xi} + \frac{\partial\phi}{\partial\theta}\frac{U(t)}{R} \qquad (21)\\ \left(\frac{\partial\phi}{\partial t}\right)_{stator} &= \frac{U_d}{R}\frac{\partial\phi}{\partial\xi}, \qquad (22)\end{aligned}$$

where the unsteadiness of the flow through the stator passage reflects the accelerations associated with transients effects. For the rotor there is also unsteadiness due to the rotor blades moving with velocity $U(t)$ through a circumferential nonuniform flow. Considering a compressor of N stages, we get

$$\frac{p_E - p_1}{\frac{1}{2}\rho U^2} = NF(\phi) - \frac{1}{2a}\left(2\frac{\partial\phi}{\partial\xi} + \frac{U}{U_d}\frac{\partial\phi}{\partial\theta}\right), \tag{23}$$

where

$$a \triangleq \frac{R}{N\tau U_d} \tag{24}$$

is a constant. Note that if $U(\xi) = \text{const}$ and $U_d \equiv U$ such that $\xi = \xi_{MG}$, equation (23) is reduced to equation (5) in [11]. It is noted that the flow coefficient ϕ can depend on both ξ and θ, even though the atmospheric stagnation pressure p_T is constant. The average of ϕ around the wheel is defined as

$$\frac{1}{2\pi}\int_0^{2\pi}\phi(\xi,\theta)d\theta \triangleq \Phi(\xi). \tag{25}$$

Further

$$\phi = \Phi(\xi) + g(\xi,\theta) \text{ and } h = h(\xi,\theta), \tag{26}$$

where h is a circumferential coefficient.

3.3 Entrance duct and guide vanes

The fact that the rotational speed of the wheel now is assumed time varying does not change the conditions upstream of the compressor. Therefore the equations stated in [11] are still valid, and will be presented here. The pressure difference over the IGVs, where the flow is axial, can be written

$$\frac{p_1 - p_0}{\rho U^2} = \frac{1}{2} K_G h^2, \tag{27}$$

where $0 < K_G \leq 1$ is the entrance recovery coefficient. If the IGVs are lossless $K_G = 1$. Upstream of the IGV irrotational flow is assumed so that a (unsteady) velocity potential $\tilde{\phi}$ exists. The gradient of $\tilde{\phi}$ gives axial and circumferential velocity coefficients everywhere in the entrance duct. At the IGV entrance point (denoted by subscript '0') we have

$$(\tilde{\phi}_\eta)_0 = \Phi(\xi) + g(\xi, \theta) \text{ and } (\tilde{\phi}_\theta)_0 = h(\xi, \theta), \tag{28}$$

where partial derivation wrt η and θ is denoted by subscripts. Applying Bernoulli's equation we get

$$\frac{p_T - p_0}{\rho U^2} = \frac{1}{2}(\phi^2 + h^2) + (\tilde{\phi}_\xi)_0, \tag{29}$$

where the term $(\tilde{\phi}_\xi)_0$ is due to unsteadiness in Φ and g. A straight inlet duct of nondimensional length l_I is considered, and the velocity potential can be written

$$\tilde{\phi} = (\eta + l_I)\Phi(\xi) + \tilde{\phi}'(\xi, \eta), \tag{30}$$

where $\tilde{\phi}'$ is a disturbance velocity potential such that

$$\tilde{\phi}'\Big|_{\eta = -l_I} = 0 \text{ , } (\tilde{\phi}'_\eta)_0 = g(\xi, \theta) \text{ and } (\tilde{\phi}'_\theta)_0 = h(\xi, \theta). \tag{31}$$

Equation (29) can now be written

$$\frac{p_T - p_0}{\rho U^2} = \frac{1}{2}(\phi^2 + h^2) + l_I \frac{d\Phi}{d\xi} + (\tilde{\phi}'_\xi)_0. \tag{32}$$

3.4 Exit ducts and guide vanes

Downstream of the compressor the flow is complicated and rotational. As in [11], the pressure p in the exit duct is assumed to differ only slightly from the static plenum pressure $p_s(\xi)$, such that the pressure coefficient P satisfies Laplace's equation.

$$P \triangleq \frac{p_s(\xi) - p}{\rho U^2} \text{ , } \nabla^2 P = 0. \tag{33}$$

The axial Euler equation [12] is used to find the pressure drop across the exit duct. Generally we have in the x-coordinate

$$-\frac{dp}{dx} = \rho \frac{dC_x}{dt}, \tag{34}$$

where C_x is the velocity component along the x-axis, the axial flow velocity. Employing the chosen nondimensionalization of time and distance,

$$\frac{d}{dt} = \frac{U_d}{R}\frac{d}{d\xi} \text{ and } \frac{d}{dx} = \frac{1}{R}\frac{d}{d\eta}, \tag{35}$$

we get

$$\frac{dp_E}{dx} = -\rho U^2 \frac{1}{R}(P_\eta)_E \tag{36}$$

$$\frac{dC_x}{dt} = \frac{U_d}{R}\frac{d}{d\xi}\left\{(\tilde{\phi}_\eta)_0 U\right\}. \tag{37}$$

Inserting (36) and (37) in (34) we get the following expression for axial Euler equation, evaluated at E, where time varying U has been taken into account

$$\begin{aligned}(P_\eta)_E &= \frac{U_d}{U^2}\frac{d}{d\xi}\left\{(\tilde{\phi}_\eta)_0 U\right\} \\ &= \frac{U_d}{U^2}\left[(\tilde{\phi}_{\eta\xi})_0 U + (\tilde{\phi}_\eta)_0 \frac{dU}{d\xi}\right]. \end{aligned}\tag{38}$$

From (28) we have

$$(\tilde{\phi}_{\eta\xi})_0 = \Phi_\xi(\xi) + (\tilde{\phi}'_{\eta\xi})_0. \tag{39}$$

Inserting (28) and (39) into (38) we get

$$(P_\eta)_E = \frac{U_d}{U}\left[\frac{d\Phi}{d\xi} + (\tilde{\phi}'_{\eta\xi})_0\right] + \frac{U_d}{U^2}\frac{dU}{d\xi}\left[\Phi(\xi) + (\tilde{\phi}'_\eta)_0\right]. \tag{40}$$

We want that $P = 0$ for at the duct exit. Thus,

$$\begin{aligned} P &= \frac{U_d}{U(\xi)}\left[(\eta - l_E)\frac{d\Phi}{d\xi} - \tilde{\phi}'_\xi\right] \\ &\quad + \frac{U_d}{U^2}\frac{dU}{d\xi}\left[(\eta - l_E)\Phi(\xi) - \tilde{\phi}'\right]. \end{aligned}\tag{41}$$

Finally we get

$$\begin{aligned}\frac{p_s - p_E}{\rho U^2} &= (P)_E = \frac{U_d}{U(\xi)}\left[-l_E \frac{d\Phi}{d\xi} - (m-1)(\tilde{\phi}'_\xi)_0\right] \\ &\quad + \frac{U_d}{U^2}\frac{dU}{d\xi}\left[-l_E \Phi(\xi) - (m-1)(\tilde{\phi}')_0\right], \end{aligned}\tag{42}$$

where, as in [10] and [11], the compressor duct flow parameter m has been included. It is noted that if $U(\xi)$ =const and $U_d \equiv U$ such that $\xi = \xi_{MG}$, equation (42) is reduced to equation (20) in [11].

3.5 Overall pressure balance

Using the preceding calculations, we now want to calculate the net pressure rise from the upstream reservoir total pressure p_T to the plenum static pressure p_s at the discharge of the exit duct. This is done by combining equations (23), (27), (32) and (42) according to

$$\begin{aligned}\frac{p_s - p_T}{\rho U^2} &= (NF(\phi) - \frac{1}{2}\phi^2) - (l_I + l_E\frac{U_d}{U} + \frac{1}{a})\frac{d\Phi}{d\xi} \\ &\quad + \left((1-m)\frac{U_d}{U} - 1\right)(\tilde{\phi}'_\xi)_0 - \frac{1}{2}(1 - K_G)h^2 \\ &\quad + \frac{U_d}{U^2}\frac{dU}{d\xi}\left(-l_E\Phi(\xi) - (m-1)(\tilde{\phi}')_0\right) \\ &\quad - \frac{1}{2a}\left(2(\tilde{\phi}'_{\xi\eta})_0 + \frac{U}{U_d}(\tilde{\phi}'_{\eta\theta})_0\right), \end{aligned}\tag{43}$$

where

$$\begin{aligned} 2\frac{\partial\phi}{\partial\xi} + \frac{\partial\phi}{\partial\theta} &= 2\frac{\partial\Phi}{\partial\xi} + 2\frac{\partial g}{\partial\xi} + \frac{\partial g}{\partial\theta} \\ &= 2\frac{\partial\Phi}{\partial\xi} + 2(\tilde{\phi}'_{\xi\eta})_0 + (\tilde{\phi}'_{\eta\theta})_0 \end{aligned}\tag{44}$$

has been used. By defining [1]

$$\Psi(\xi) = \frac{p_s - p_T}{\rho U^2} \text{ , } \psi_c(\phi) = NF(\phi) - \frac{1}{2}\phi^2 \tag{45}$$

$$l_c(U) = l_I + l_E\frac{U_d}{U} + \frac{1}{a} \text{ , } m_U(U) = (1-m)\frac{U_d}{U} - 1,$$

and assuming $K_G \equiv 1$, (43) can be written

$$\begin{aligned}\Psi(\xi) &= \psi_c(\phi) - l_c(U)\frac{d\Phi}{d\xi} + m_U(U)(\tilde{\phi}'_\xi)_0 \\ &\quad + \frac{U_d}{U^2}\frac{dU}{d\xi}\left(-l_E\Phi(\xi) - (m-1)(\tilde{\phi}')_0\right) \\ &\quad - \frac{1}{2a}\left(2(\tilde{\phi}'_{\xi\eta}) + \frac{U}{U_d}(\tilde{\phi}'_{\eta\theta})\right)_0, \end{aligned}\tag{46}$$

[1] Notice that $l_c \neq L_c R$. As in [2] L_c used in the definition of B is a constant. See equation (5).

which, with the usual assumptions, reduces to equation (26) in [11]. Equation (46) requires knowledge of the disturbance velocity potential $\tilde{\phi}'$ and its derivatives. As $\tilde{\phi}'$ satisfies Laplace's equation, $\nabla^2\tilde{\phi}' = 0$, it has a Fourier series. As an approximation only the first term of this series is used, which means

$$(\tilde{\phi}'_\eta)_0 = -(\tilde{\phi}'_{\theta\theta})_0. \quad (47)$$

Switching notation to

$$Y(\xi,\theta) \stackrel{\triangle}{=} (\tilde{\phi}')_0 \;\Rightarrow\; (\tilde{\phi}'_\eta)_0 = -Y_{\theta\theta}, \quad (48)$$

equation (46) is written

$$\begin{aligned}\Psi(\xi) &= \psi_c(\Phi - Y_{\theta\theta}) - l_c(U)\frac{d\Phi}{d\xi} + m_U(U)Y_\xi \\ &+\frac{U_d}{U^2}\frac{dU}{d\xi}\left(-l_E\Phi(\xi) - (m-1)Y(\xi,\theta)\right) \\ &-\frac{1}{2a}\left(2Y_{\xi\theta\theta} + \frac{U}{U_d}Y_{\theta\theta\theta}\right). \end{aligned} \quad (49)$$

We now want to express equation (49) in terms of varying B instead of varying U. Using (5) it is seen that

$$\begin{aligned}\Psi(\xi) &= \psi_c(\Phi - Y_{\theta\theta}) - l_c(B)\frac{d\Phi}{d\xi} + m_B(B)Y_\xi \\ &+\frac{U_d\Gamma\Lambda_1}{b}\left(-l_E\Phi(\xi) - (m-1)Y(\xi,\theta)\right) \\ &-\frac{1}{2a}\left(2Y_{\xi\theta\theta} + \frac{bB}{U_d}Y_{\theta\theta\theta}\right). \end{aligned} \quad (50)$$

Integrating (50) over one cycle wrt θ we get

$$\Psi(\xi)+l_c(B)\frac{d\Phi}{d\xi}+l_E\frac{U_d\Gamma\Lambda_1}{b}\Phi(\xi) = \frac{1}{2\pi}\int_0^{2\pi}\psi_c(\Phi-Y_{\theta\theta})d\theta. \quad (51)$$

3.6 Plenum mass balance

The mass balance in the plenum can be written

$$\frac{d}{dt}(\rho_p V_p) = m_c - m_t, \quad (52)$$

where ρ_p is the plenum density, m_c is the mass flow entering the plenum from the compressor, and m_t is the mass flow leaving through the throttle. Assuming the pressure variations in the plenum isentropic, we have

$$\frac{dp_p}{dt} = \frac{a_s^2}{V_p}(m_c - m_t). \quad (53)$$

By nondimensionalizing pressure with ρU^2, mass flow with $\rho U A_c$, transforming to nondimensional time ξ, and taking account for (5), (53) can be written

$$\frac{d\Psi}{d\xi} = \frac{\Lambda_2}{B}(\Phi - \Phi_T) - \frac{2}{B}\frac{dB}{d\xi}\Psi, \quad (54)$$

where

$$\Lambda_2 = \frac{R}{L_c U_d}b. \quad (55)$$

Using (10) we get

$$\frac{d\Psi}{d\xi} = \frac{\Lambda_2}{B}(\Phi - \Phi_T) - 2\Lambda_1\Gamma B\Psi. \quad (56)$$

The model of the compression system now consists of the torque balance for the spool (10), the local momentum balance (50), the annulus averaged momentum balance (51) and the mass balance of the plenum (56).

3.7 Characteristics

The compression systems characteristics are taken from [11]. The usual 3rd order polynomial steady state compressor characteristic is employed:

$$\psi_c(\phi) = \psi_{c0}+H\left(1+\frac{3}{2}(\frac{\phi}{W}-1)-\frac{1}{2}(\frac{\phi}{W}-1)^3\right), \quad (57)$$

where the parameters ψ_{c0}, H and W are defined in [11]. The compressor characteristic can also be plotted as a family of curves, one line for each rotational speed, with the surge line passing through the local maxima of the constant speed lines. However, when using the nondimensionalizing employed here , these lines collapse into a single curve $\psi_c(\phi)$ [2], and the surge line collapses into the local maximum $\psi_c(\phi)$. When the compressor is in rotating stall the characteristic is given by

$$\psi_s(\phi) = \psi_{c0}+H\left(1-\frac{3}{2}(\frac{\phi}{W}-1)+\frac{5}{2}(\frac{\phi}{W}-1)^3\right). \quad (58)$$

The throttle characteristics is taken to be

$$\Phi_T = \gamma\sqrt{\Psi}. \quad (59)$$

3.8 Galerkin procedure

As previously assumed Y is approximated with the first term in a Fourier series, that is Y is represented by a single harmonic function Y^* of unknown time varying amplitude $A(\xi)$:

$$Y^* = WA(\xi)\sin(\theta - r(\xi)), \quad (60)$$

where $r(\xi)$ is an unknown phase angle. From (50), we get

$$\begin{aligned}Y_\xi &= \frac{1}{m_B(B)}\Bigg(\Psi(\xi) + l_c(B)\frac{d\Phi}{d\xi} + l_E\frac{U_d\Gamma\Lambda_1}{b}\Phi(\xi) \\ &-\psi_c(\Phi - Y_{\theta\theta}) + \frac{U_d\Gamma\Lambda_1}{b}(m-1)Y(\xi,\theta) \\ &-\frac{1}{2a}\left(2Y_{\xi\theta\theta} + \frac{bB}{U_d}Y_{\theta\theta\theta}\right)\Bigg) \end{aligned} \quad (61)$$

Defining $\zeta = \theta - r(\xi)$, we get from (60)

$$Y^*_\xi = W\frac{dA}{d\xi}\sin\zeta - WA(\xi)\cos\zeta\frac{dr}{d\xi}. \quad (62)$$

The model developed thus far includes partial derivatives of Y. A Galerkin approximation is to be used to produce a set of ordinary differential equations. A residue R, is defined as

$$R \stackrel{\triangle}{=} Y^*_\xi - Y_\xi. \quad (63)$$

The Galerkin approximation is calculated using the weight functions

$$h_1 = 1,\; h_1 = \sin\zeta,\; h_2 = \cos\zeta \quad (64)$$

and the inner product

$$\langle R, h_i\rangle = \frac{1}{2\pi}\int_0^{2\pi} R(\zeta)h_i(\zeta)d\zeta. \quad (65)$$

Calculating $\langle R, h_i\rangle = 0$ for $i = 1,2,3$ and using (57) give after some lengthy algebra

$$\begin{aligned}\frac{1}{2\pi}\int_0^{2\pi}\psi_c(\phi)d\zeta &= \Psi(\xi) + l_c(B)\frac{d\Phi}{d\xi} + l_E\frac{U_d\Gamma\Lambda_1}{b}\Phi(\xi) \\ \frac{1}{\pi W}\int_0^{2\pi}\psi_c(\phi)\sin\zeta d\zeta &= \frac{U_d\Gamma\Lambda_1(m-1)}{b}A(\xi) + \frac{dA}{d\xi}m'_B \\ \frac{1}{\pi W}\int_0^{2\pi}\psi_c(\phi)\cos\zeta d\zeta &= -(\frac{dr}{d\xi}m'_B - \frac{bB}{2aU_d})A(\xi), \end{aligned} \quad (66)$$

where $m'_B = (\frac{1}{a} - m_B)$ and $\phi = \Phi + WA(\xi)\sin\zeta$. Examining the last equation in (66), it is recognized that the integral vanishes, and assuming $A \neq 0$ the phase angle r satisfies

$$\frac{dr}{d\xi} = \frac{\frac{1}{2}\frac{b}{U_d}}{1 - m_B(B)a}B \qquad (67)$$

Notice that time varying B implicates that the phase angle r is not a constant, which was the case in [11].

3.9 Final model

By evaluating the integrals in (66), using (10), (54) and rearranging, we get the following model for the compression system

$$\frac{d\Phi}{d\xi} = \frac{H}{l_c(B)}\left(-\frac{\Psi - \psi_{c0}}{H} + 1 + \frac{3}{2}(\frac{\phi}{W} - 1)(1 - \frac{J}{2}) - \frac{1}{2}(\frac{\phi}{W} - 1)^3 - \frac{l_E U_d \Gamma \Lambda_1}{bH}\Phi\right) \qquad (68)$$

$$\frac{d\Psi}{d\xi} = \frac{\Lambda_2}{B}(\Phi - \Phi_T) - 2\Lambda_1 \Gamma B \Psi \qquad (69)$$

$$\frac{dJ}{d\xi} = J\left(1 - (\frac{\phi}{W} - 1)^2 - \frac{J}{4} - \frac{2U_d\Gamma\Lambda_1(m-1)W}{3bH}\right)\frac{3aH}{(1 - m_B a)W} \qquad (70)$$

$$\frac{dB}{d\xi} = \Lambda_1 \Gamma B^2 = \Lambda_1(u - \tau_c)B^2 \qquad (71)$$

where J is defined as the square of the stall amplitude

$$J(\xi) \triangleq A^2(\xi), \qquad (72)$$

and $u = \tau_t$ is the speed control. The model (68) is in the desired form of (1). Notice that the model is highly coupled, so that an acceleration of U should have impact on all states. It should be noted that the model developed in this paper can be reduced to other well known compression system models. This is summed up in table 2.

Changes made to (68)-(71)	Redefine nondim. time acc. to	Gives the model of
$J \equiv 0$, $\frac{dB}{d\xi} = 0$ $U = U_d$, $\Gamma = 0$	$\xi := \frac{Ut}{R}$	Greitzer [6]
$\frac{dB}{d\xi} = 0$, $U = U_d$ $\Gamma = 0$	$\xi := \frac{Ut}{R}$	Moore/Greitzer [11]
$J \equiv 0$	$\xi := t\omega_H$	Fink et.al. [2]

Table 2: Relation with other models. (ω_H is the Helmholtz frequency)

4 Simulations

Here some simulations of the model will be presented. For speed control, a simple P-type controller of the form

$$\Gamma_t = c(U_d - U), \qquad (73)$$

will be used. The nondimensional drive torque Γ_t is used as the control, and feedback from compressor speed U is assumed. Initial values were chosen as

$$(\Phi_0\ \Psi_0\ J_0\ B_0) = (0.55\ 0.65\ 0.05\ 0.1), \qquad (74)$$

such that the (Φ, Ψ)-trajectory starts on the stable part of the compressor characteristic as can be seen in figure 2. In [5] compressor speed was controlled in a similar manner, and stability was proven using Lyapunovs theorem. Work on this subject for the model (68)-(71) is underway. The desired speed was set to $U_d = 215$m/s in both the following simulations. Numerical values for the parameters in the model are given in appendix A.

4.1 Unstable equilibrium, $\gamma = 0.5$

In figure 2, a simulation of the system is shown. The throttle gain was set at $\gamma = 0.5$ so that the equilibrium is to the left of the local maximum of the characteristic. As can be seen from figure 2, the compressor goes into rotating stall as B (and thus compressor speed U) is low. Moreover, when the applied torque from the speed controller cause B to increase, the stall amplitude J falls off and the compressor goes into surge. This is what could be expected according to [7]. The surge oscillations have a period of $\xi \approx 180$, which correspond to a surge frequency of about 10Hz. A desired speed of $U_d = 215$ corresponds to a desired B-parameter of $B_d = U_d/b = 2.23$. After $\xi \approx 1500$ this value is reached. As the compressor torque Γ_c varies with ϕ, see equation (17), we would expect oscillations in speed U as the compressor is in surge. This is confirmed by the lower right plot in figure 2. In the upper plot of figure 3, the trajectory starts on the stable part of the characteristic, then rotating stall occurs and the trajectory approaches the intersection of the throttle and in-stall characteristics. As B increases the resulting surge oscillations are clearly visible.

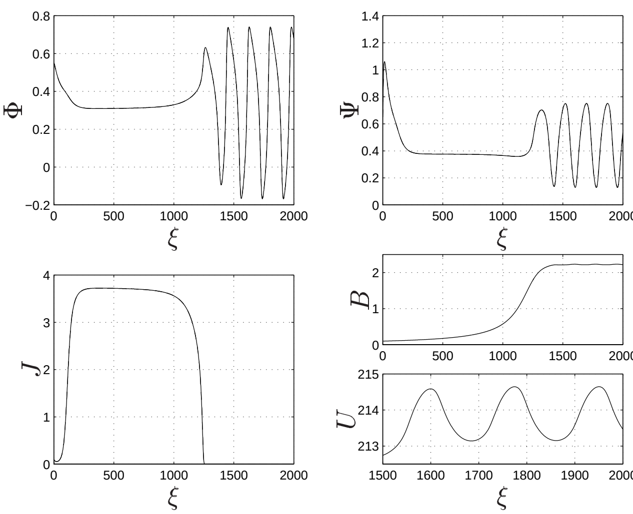

Figure 2: Simulation of the system (68)-(71). Low B leads to rotating stall, and high B leads to surge.

4.2 Stable equilibrium $\gamma = 0.65$

In figure 4, the impact of the spool dynamics on a stable equilibrium of the compression system is illustrated. Initial values were unchanged. The throttle gain was set at $\gamma = 0.65$, giving a stable equilibrium, and the speed controller gain was chosen as $c = 1$. The dotted trajectories show the system response to a speed change from $U = 0.05$ to $U = 215$. It can be seen that the acceleration of U affects the other states of the model. This is due to the couplings with speed U and torque Γ in the model. Of special interest is the stall amplitude. The initial value of $J(0) = 0.05$ grows to nearly fully developed rotating stall as the machine is accelerating, but is quickly damped out as desired speed is reached. The response is also plotted in the lower plot of figure 3. Simulations show that this stalling can be avoided by accelerating the compressor at a lower rate, that is by

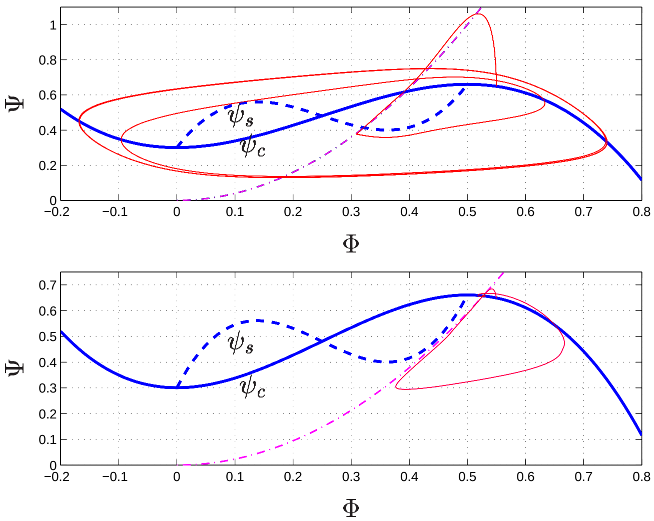

Figure 3: Simulations result superimposed on the compression system characteristics. The compressor characteristic, the in-stall characteristic and the throttle characteristic are drawn with solid, dashed and dash-dot lines respectively.

using a smaller c.

In contrast, the solid trajectories in figure 4 show the response without the spool dynamics. Now, the initial value $J(0) = 0.05$ is damped out very quickly, and Φ and Ψ converges to their equilibrium values. The only transient effects are due to the initial conditions.

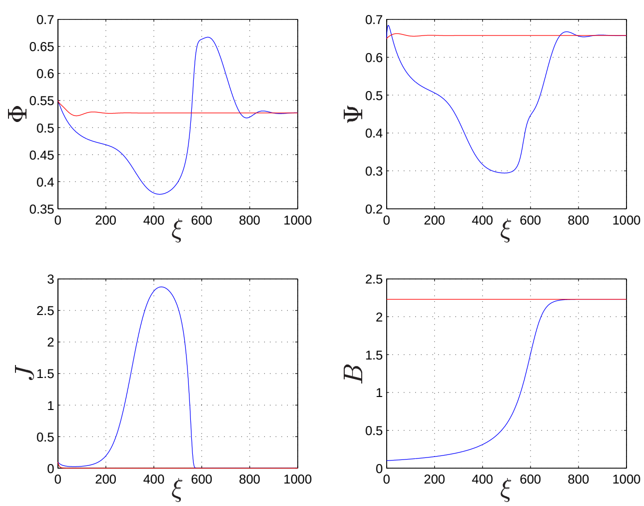

Figure 4: Stable equilibrium with and without B-dynamics

5 Conclusion and further work

A Moore-Greitzer axial compressor model with spool dynamics has been derived. This results in a model with time varying B-parameter. Through simulations it has been demonstrated that the model is capable of demonstrating both rotating stall and surge, and that the type of instability depends on the compressor speed. Compressor speed was controlled with a simple proportional control law. Further work includes 1) Stability analysis and stall/surge control design for variable speed compressors, 2) The use of both speed control and stall/surge control to achieve rapid acceleration without stalling, and 3) Inclusion of higher harmonics in rotating stall, that is include more terms in the Fourier series of $\tilde{\phi}'$. This will be the subject of future publications.

A Numerical values used in simulations

Sym.	value	Sym.	value	Sym.	value
R	0.1m	ρ	$1.15\frac{\text{kg}}{\text{m}^3}$	a_s	$340\frac{\text{m}}{\text{s}}$
l_E	8	l_I	2	L_c	3m
V_p	1.5m^3	A_c	0.01m^2	a	0.3
H	0.18	W	0.25	ψ_{c0}	0.3
I	0.03kgm^2	m	1.75	σ	0.9

Table 3: Compression system parameters used in simulations

References

[1] B. de Jager. Rotating stall and surge control : A survey. In *Proceedings of the 35th Conference on Decision and Control*, pages 1857–1862, New Orleans, LA, 1995.

[2] D.A. Fink, N.A. Cumpsty, and E.M. Greitzer. Surge dynamics in a free-spool centrifugal compressor system. *Journal of Turbomachinery*, 114:321–332, 1992.

[3] J.T. Gravdahl and O. Egeland. Compressor surge control using a close-coupled valve and backstepping. In *Proceedings of the 1997 American Control Conference*, Albuquerque, NM, June 1997.

[4] J.T. Gravdahl and O. Egeland. Control of the three-state Moore-Greitzer compressor model using a close-coupled valve. In *Proceedings of the 1997 European Control Conference*, July 1997.

[5] J.T. Gravdahl and O. Egeland. Speed and surge control for a low order centrifugal compressor model. Accepted as a regular paper to 1997 IEEE Conference on Control Applications, October 1997.

[6] E.M. Greitzer. Surge and Rotating stall in axial flow compressors, Part I: Theoretical compression system model. *Journal of Engineering for Power*, 98:190–198, 1976.

[7] E.M. Greitzer and F.K. Moore. A theory of post-stall transients in a axial compressor systems: Part II–Application. *Journal of Engineering for Gas Turbines and Power*, 108:231–239, 1986.

[8] K.E. Hansen, P. Jørgensen, and P.S. Larsen. Experimental and theoretical study of surge in a small centrifugal compressor. *Journal of Fluids Engineering*, 103:391–394, 1981.

[9] J.D. Mattingly. *Elements of gas turbine propulsion*. McGraw-Hill series in aeronautical and aerospace engineering. McGraw-Hill, 1996.

[10] F.K. Moore. A theory of rotating stall of multistage axial compressors: Parts I,II,III. *J. of Engineering for Gas Turbines and Power*, 106:313–336, 1984.

[11] F.K. Moore and E.M. Greitzer. A theory of post-stall transients in a axial compressor systems: Part I–Development of equations. *Journal of Engineering for Gas Turbines and Power*, 108:68–76, 1986.

[12] F.M. White. *Fluid mechanics*. McGraw-Hill, New York, 2nd edition, 1986.